Temperature-Induced Morphology Control in the Polymer-Foaming Process

L. J. M. Jacobs, M. F. Kemmere, and J. T. F. Keurentjes
Process Development Group, Dept. of Chemical Engineering and Chemistry, Eindhoven University of Technology, 5600 MB Eindhoven, The Netherlands

Ch. A. Mantelis, and Th. Meyer
Groupe des Procédés Macromoléculaires, Ecole Polytechnique Fédérale de Lausanne, Station 6, CH-1015 Lausanne, Switzerland

DOI 10.1002/aic.11273
Published online August 27, 2007 in Wiley InterScience (www.interscience.wiley.com).

Supercritical carbon dioxide ($scCO_2$) is a promising foaming agent for the production of polymeric foams, representing an environmentally friendly alternative for the foaming agents currently used. During the expansion phase of the $scCO_2$-foaming process, temperature plays an essential role. This study focuses on relating the effects of temperature and pressure profiles on the foaming process and the resulting foam morphology. Therefore, several experiments have been performed in a high pressure reaction calorimeter (RC1e) that can be set to three different modes: isothermal, adiabatic, and isoperibolic. It has been observed that the foaming could be divided into four stages: nucleation, slow cell growth, fast cell growth, and shrinkage. The degree of shrinking that occurs is for a great deal dependent on the exposure to higher temperatures at the end of the foaming process. Since shrinkage does not occur in the adiabatic mode, this mode gives the best control on the foam morphology. © 2007 American Institute of Chemical Engineers *AIChE J,* 53: 2651–2658, 2007
Keywords: foam, polymer processing, supercritical processes, process control, nucleation

Introduction

The application of micro and macrocellular foams include thermal and electrical insulation, sports gear, packaging and wrapping materials, absorbents, separation membranes, and catalytic supports. The most common techniques to produce these foams is by thermally induced phase separation (TIPS) and by the use of chemical-foaming agents in the extrusion of rubbers.[1] However, these methods can lead to substantial emissions of volatile organic compounds (VOCs) to the environment. Currently, governmental regulations are forcing the industry to replace organic-foaming agents with more environmentally friendly alternatives. For this reason, the application of supercritical carbon dioxide ($scCO_2$) for the production of polymeric foams is being explored.[2–8]

In principle, the CO_2-foaming process can be regarded as the saturation of a polymer at a certain temperature and CO_2 pressure, followed by a (rapid) depressurization step. Upon depressurization, the CO_2 in the polymer becomes oversaturated. As a consequence, phase separation and nucleation occurs, and subsequently the created nuclei grow into cells, defining the foam morphology. Figure 1 gives a schematic representation of the foaming process. It is clear that the saturation temperature and pressure, together with the depres-

Correspondence concerning this article should be addressed to L. J. M. Jacobs at l.j.m.jacobs@tue.nl.

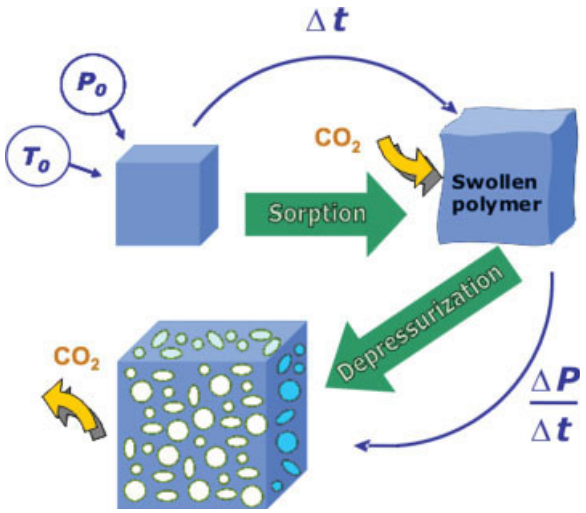

Figure 1. Schematic representation of the foaming process using $scCO_2$.

[Color figure can be viewed in the online issue, which is available at www.interscience.wiley.com.]

surization rate have a major influence on the resulting foam morphology.

Furthermore, the temperature during the depressurization step and specific polymer properties such as the affinity for CO_2 and the glass transition temperature play an important role in the foaming process. The affinity determines the amount of CO_2 that can dissolve into the polymer,[9] and this mainly governs the driving force for cell growth. An additional effect of the sorption of CO_2 into the polymer is the so-called plasticization of the polymer: when the concentration of CO_2 in the polymer increases, the glass transition temperature (T_g) will decrease (see Figure 2).[10–12] The latter is significant for the foaming process, because the T_g determines the timeframe for cell growth.

As the temperature plays an essential role in the foaming process, it is important to know what the temperature profile will be upon depressurization and the effect the temperature profile will have on the resulting foam morphology. Therefore, experiments have been performed in a high pressure reaction calorimeter (RC1*e*) that can be set to three different modes: isothermal, adiabatic, and isoperibolic. This apparatus is extremely suited to accurately investigate different temperature profiles, since each mode results in its own unique temperature profile upon depressurization. Another advantage is that the RC1*e* can accurately measure the pressure during the depressurization step. This study focuses on relating the effects of different temperature and pressure profiles to the foaming process and the resulting foam morphology.

Experimental

High-pressure reaction calorimeter and modes of operation

In reaction calorimetry, a heat effect is measured as a function of an imposed temperature regime.[13,14] On the basis of this principle, several calorimeters have been developed to monitor chemical reactions.[15] The experimental setup used in this study was developed at the EPFL in collaboration with Mettler-Toledo GmbH to monitor reactions in supercritical fluids with emphasis on supercritical carbon dioxide.[16] The equipment consisted of a stainless steel autoclave and was designed to work at pressures and temperatures up to 350 bar and 300°C, respectively. The reactor was surrounded by a jacket to control the temperature using silicon oil. The jacket was coupled to an RC1*e* calorimeter, which measured and controlled the jacket temperature. Additionally, the temperature of the reactor flange and cover were measured and controlled, since in the case of supercritical fluids both pieces come into direct contact with the reactor content, and their temperature contributes to the occurring heat flows in the reactor. A schematic representation of the setup is shown in Figure 3.

The reactor also permitted visual observation of its contents through three sapphire windows, for which two were used to light the reactor and one was used for observation with an endoscope. The image was transported digitally and could be recorded either continuously or in separate photos.

The software provided with the calorimeter (WinRC) contained three preprogrammed modes of operation, i.e., isothermal, adiabatic, and isoperibolic. In the first mode, the temperature of the jacket was altered in such a way that the reactor temperature always equaled the set value. In the adiabatic mode, the jacket temperature followed accurately the reactor temperature, resulting in zero heat flow through the reactor jacket. In the isoperibolic mode, the jacket temperature was set and the reactor temperature was left uncontrolled to respond to the thermal phenomena in the reactor, such as the carbon dioxide expansion due to depressurization. It must be noted that in all of the above modes, the temperature of the reactor cover and the reactor flange were also controlled and were set equal to the reactor temperature. Therefore, minimal heat flow can be approximated through these two pieces of the reactor.

Accurate temperature measurements (±0.05°C) were performed to monitor the temperature profiles upon depres-

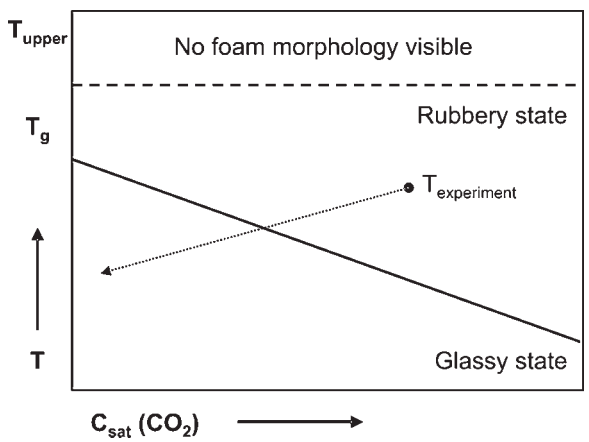

Figure 2. Schematic representation of the temperature conditions that need to be fulfilled to foam polymers using $scCO_2$.

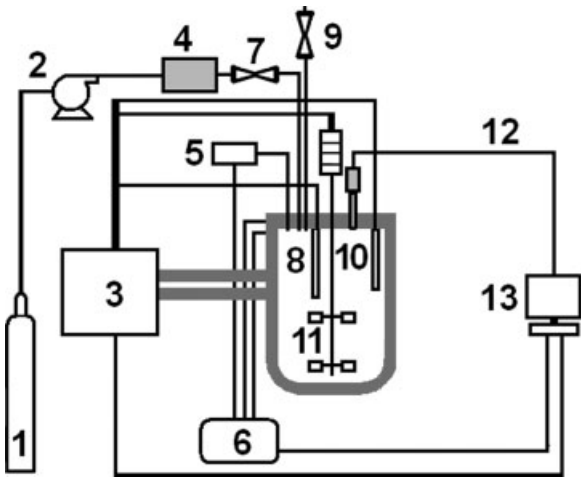

Figure 3. Schematic representation of the experimental setup of the high pressure reaction calorimeter.

(1) CO_2 cylinder, (2) pump, (3) RC1*e* calorimeter, (4) coriolis mass flow meter, (5) pressure sensor, (6) RD10 controller, (7) valve, (8) PT100, (9) depressurization valve, (10) calibration heater, (11) magnetic stirrer, (12) digital camera, and (13) PC.

surization of CO_2 in the reactor during the foaming experiments.

Materials

Polystyrene (PS), poly(styrene-*co*-methyl methacrylate) (SMMA) with 40 wt % styrene, and poly(methyl methacrylate) (PMMA) were purchased from Aldrich Chemical Company. The molecular weights (M_w) of the polymers were 259, 150, and 120 kg/mol for PS, SMMA, and PMMA, respectively. The glass transition temperature (T_g) as determined by DSC analysis (PerkinElmer Pyris Diamond DSC) revealed a T_g of 99, 104, and 103°C for PS, SMMA, and PMMA, respectively. Carbon dioxide (quality 30) was obtained from Carbagas (Switzerland) and used without further purification.

Depressurization and foaming experiments

For both the depressurization and foaming experiments, accurate measurements of the temperature profile upon depressurization were performed in the reaction calorimeter. First, a set of depressurization experiments were performed without polymer present in the reactor. Here, the RC1*e* was pressurized with CO_2 at a precisely set temperature and pressure (±0.1°C and ±0.05 bar, respectively) and subsequently depressurized, by opening a micrometric SITEC needle valve between 2.5 and 3.2 turns (9.5 turns to fully open). This resulted in a change of the depressurization time between 15 and 50 min and therefore in a change in the depressurization rate. The experiments were performed in the isothermal, adiabatic, and isoperibolic mode, and the results obtained were used as a calibration of the temperature profiles upon depressurization for the foaming experiments. These experiments are referred to as the calibration experiments.

To standardize the foaming experiments, the polymers used were pressed at high temperature (160°C) and pressure (200 bar) into discs with a thickness of 3 mm and a diameter of 2 cm. During the foaming experiments, the polymeric disc was placed in the reactor and afterward the reactor was pressurized with CO_2 at a precisely set saturation temperature and pressure (±0.1°C and ±0.05 bar, respectively). It is important to note that the disc was placed into the CO_2 flow and did not touch any metallic parts of the reactor. Once the discs were saturated the foam was produced by expansion of CO_2 inside the pressurized vessel. The applied experimental conditions are given in Tables 1 and 2.

The density of the produced foams was determined using a pycnometer, where the difference of the weight of the pycnometer and water with and without the polymeric foam was used to calculate the volume of the beforehand weighed sample.

Results and Discussion

Calibration experiments

Figure 4 shows the reactor temperature and pressure profiles in the isothermal mode. Because of the expanding CO_2, the temperature of the reactor (T_r) decreases. The calorimeter attempts to counteract the decrease in temperature by increasing the jacket temperature (T_j), which results in an increase in the reactor temperature. It can be seen that the temperature of the reactor oscillates and eventually stabilizes, which takes about 10–20 min depending on the depressurization rate. The faster the depressurization rate, the more the temperature decreases, the longer it takes for T_r to stabilize. Furthermore, the control parameters of the WinRC have been optimized for $scCO_2$. The faster the depressurization rate, the sooner the CO_2 enters the gas phase, which hampers the calorimeter to control the temperature.

In the adiabatic mode, the jacket follows the reactor temperature instead of trying to keep the temperature constant, as in the isothermal mode. Therefore, a decrease of T_r is not counteracted, and the temperature continues to decrease as can be seen in Figure 5. The higher the depressurization rate, the more the temperature decreases. The slight increase in T_r at the end of the slow depressurization at 2.5 turns is attributed to two factors. Because of the large inertia of the reactor flange and cover, these two pieces respond more slowly to the change in T_r, resulting in a slight increase of the temperature at the end of the experiment. Secondly, the stirrer also continues to provide heat, which adds to the increase of T_r.

The temperature and pressure profiles of the isoperibolic mode are depicted in Figure 6. This mode is the most comparable to previously performed experiments,[5,17] because in those experiments the jacket does not respond to a change in T_r. A value of 117°C is set for T_j, which results in a value of 118.5°C for T_r before the depressurization step. Figure 6

Table 1. Overview of the Performed Depressurization Experiments, with the Corresponding Pressures, Temperatures, and Number of Valve Turns

200 bar 120°C	Isothermal	2.5	2.6	2.7	2.8	2.9	3.0	3.2
	Adiabatic	2.5	–	–	2.8	–	3.0	–
	Isoperibolic	2.5	–	–	2.8	–	3.0	–

Table 2. Overview of the Performed Foaming Experiments, with the Corresponding Pressures, Temperatures, and Number of Valve Turns

	SMMA			PS				PMMA	
	200 bar 120°C	200 bar 100°C	150 bar 120°C	200 bar 120°C	200 bar 100°C	150 bar 120°C	100 bar 80°C	200 bar 120°C	200 bar 100°C
Isothermal	2.5	–	–	–	–	–	–	–	–
	3.0	3.0	3.0	3.0	3.0	3.0	3.0	3.0	3.0
	3.2	–	–	–	–	–	–	–	–
Adiabatic	2.5	–	–	–	–	–	–	–	–
	3.0	–	–	–	–	–	–	–	–
	3.2	3.2	3.2	3.2	3.2	3.2	3.2	3.2	3.2
Isoperibolic	2.5	–	–	–	–	–	–	–	–
	3.0	–	–	–	–	–	–	–	–
	3.2	–	3.2	–	–	–	–	–	–

clearly shows that T_r decreases at first, once the valve has been opened. After ~3 min, T_r rises again due to the heating of the jacket. T_r decreases more at higher depressurization rates, which has also been observed in the experiments performed in the adiabatic mode. As the depressurization rate increases, the reactor has less time to heat up. Therefore, the temperature at the end of the experiment does not reach the preset value of 118.5°C.

Multistage expansion of the foaming process

After the temperature and pressure profiles of the different experimental modes were determined in the calibration experiments, several foaming experiments have been performed to determine the effect of the different modes of operation on the foaming process and the foam characteristics. The volume of the reactor is much larger when compared with the volume of the polymeric sample. Therefore, the presence of the sample will have no significant influence on the temperature and pressure profiles during the depressurization step. Hence, temperature and pressure profiles of the isothermal, adiabatic, and isoperibolic-foaming experiments are similar to those of the depressurization experiments. For that reason, Figures 4–6 also represent the temperature and pressure profiles during the expansion step of the foaming experiments.

By visual observation through the sapphire windows of the reactor, it has been possible to monitor the growth of the polymeric sample during the depressurization step. Figure 7 gives a typical sequence of events during an isoperibolic-foaming experiment saturated at 200 bar and 118.5°C, where the valve was opened 2.5 turns. These pictures show that the first nucleation takes place, because the transparent sample becomes opaque. In this first stage, which lasts for ~4–5 min, the size of the sample does not change. This means that hardly any cell growth occurs and only nucleation takes place. In the second stage, from 5 min roughly up to 20 min, the sample grows at a slow rate. During the third stage, from 20 to 40 min, the cells grow much more rapidly and the volume of the polymeric sample increases dramatically. At the end of the experiment, the sample shrinks again, indicating the beginning of a fourth stage. This last stage is more pronounced as the depressurization time increases, mainly

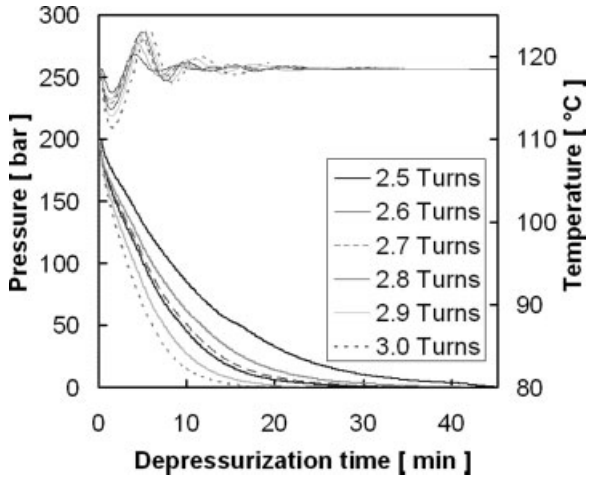

Figure 4. Temperature and pressure profiles versus time during the calibration experiments performed in isothermal mode.

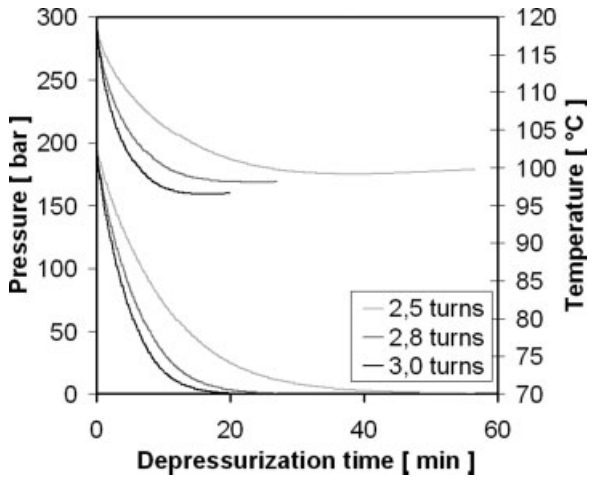

Figure 5. Temperature and pressure profiles versus time during the calibration experiments performed in adiabatic mode.

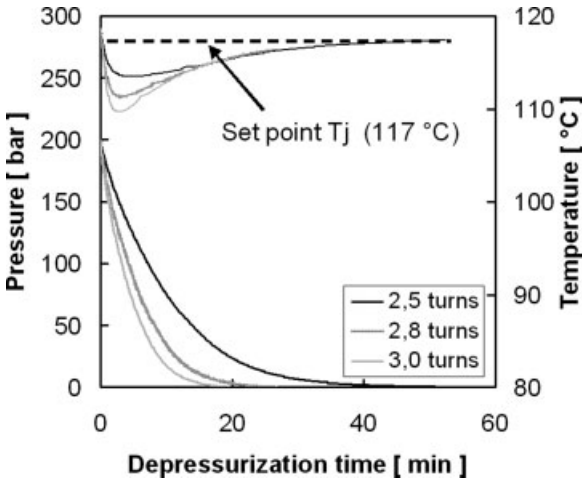

Figure 6. Temperature and pressure profiles versus time during the calibration experiments performed in isoperibolic mode.

due to the exposure of the produced foam to temperatures above the T_g of the pure polymer for a longer period of time.

When compared with the isothermal-foaming experiments, Stage 1 through 3 are also present in the adiabatic-foaming experiments. However, Stage 4 is absent in all the adiabatic experiments. This is due to the temperature decrease during the experiment, which eventually results in a temperature drop below the T_g of the pure polymer. Another consequence of this decrease is that the cell growth of the sample during the third phase is prematurely stopped. This happens because the concentration of CO_2 in the polymer decreases as the pressure in the reactor decreases, resulting in an increase of the T_g of the plasticized polymer. This phenomenon could be described as "reverse plasticization," since the opposite of the already mentioned plasticization effect takes place. As the depressurization rate increases, reverse plasticization will occur at an earlier stage, since the reactor temperature crosses the polymer T_g sooner. This leads to vitrification of the foam morphology and absence of the shrinking stage.

The fourth stage is also absent in the isothermal-foaming experiments performed at 100°C, because this temperature is very close to the T_g of the polymers used. Hence, the polymer matrix is much more rigid and the foam morphology is vitrified. This is also illustrated by comparing the densities of the isothermal foams, which is discussed in more detail in the next paragraph.

For the isoperibolic experiments, the shrinkage of the foam in the last stage is comparable to the experiments performed in the isothermal mode. As the depressurization rate decreases, the foamed polymer is exposed to higher temperatures for a longer period of time, which results in more shrinking.

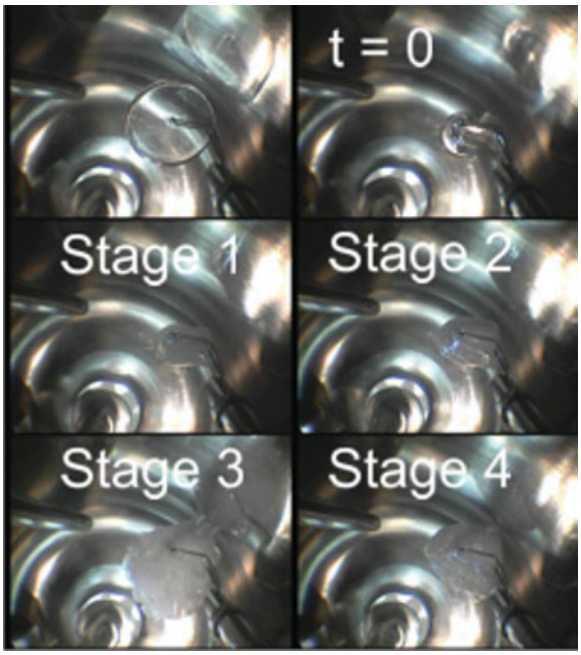

Figure 7. Picture sequence taken during the depressurization phase (valve opened 2.5 turns) of the isoperibolic-foaming experiment of SMMA, saturated at 118.5°C and 200 bar.

Stage 1: nucleation; Stage 2: slow cell growth; Stage 3: fast cell growth; Stage 4: shrinkage. [Color figure can be viewed in the online issue, which is available at www.interscience.wiley.com.]

Foam morphology due to different foaming modes

It has been shown that the mode of operation has a major effect on the imposed temperature profiles during the foaming process. As a consequence, the foam morphologies are different. Figure 8 displays the density of the produced SMMA foams versus the depressurization rate, indicated by the number of turns of the depressurizing valve and the ex-

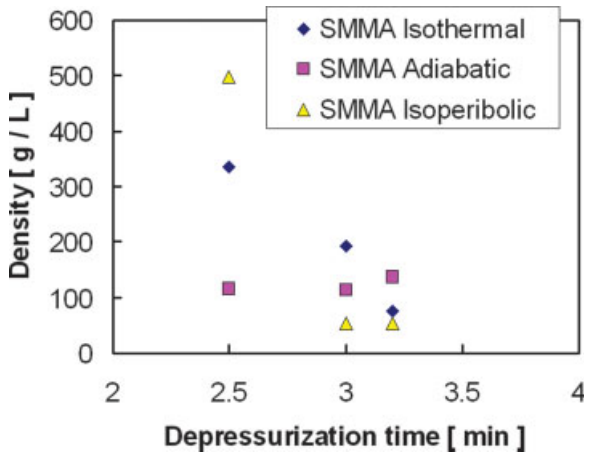

Figure 8. Density of the produced SMMA foams versus the depressurization rate in terms of the number of valve turns. Samples have been saturated at 118.5°C and 200 bar.

[Color figure can be viewed in the online issue, which is available at www.interscience.wiley.com.]

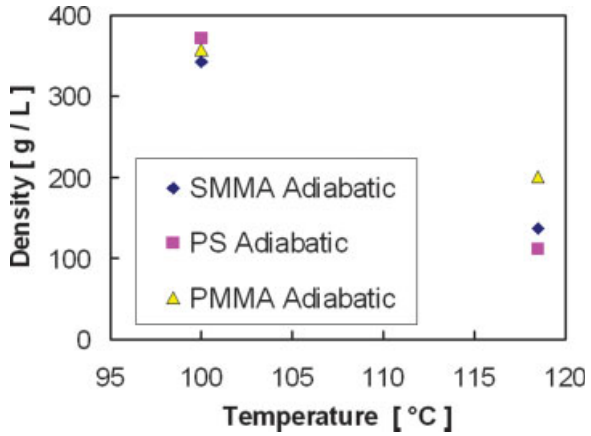

Figure 9. Densities of the produced foams versus the foaming temperature. Samples have been saturated at 200 bar and depressurized with 3.2 valve turns.

[Color figure can be viewed in the online issue, which is available at www.interscience.wiley.com.]

perimental mode. The samples have been saturated at 120°C and 200 bar. It can be seen that the density of SMMA decreases with increasing depressurization rate for both the isothermal and isoperibolic mode. Less shrinking occurs in these experiments, because the time the polymeric foam is exposed to high temperatures at the end of these experiments decreases with increasing depressurization rate, resulting in lower densities.

Figure 8 also shows that the density of the isoperibolically foamed SMMA samples at higher depressurization rates (3 and 3.2 turns) appears to remain constant at ~70 g/dm^3. Previously, several isoperibolic-foaming experiments with SMMA have been performed under similar saturation conditions, except that the depressurization times were much shorter.[17] These experiments first show an increase in density of 30–60 g/dm^3 for depressurization times ranging from less than 1–30 s. At depressurization times between 30 s and 10 min, the density of the produced foams remains more or less constant at 60–70 g/dm^3. The experiments described here with depressurization times between 15 and 50 min can be considered as an extrapolation of the previous experiments. Both sets of experiments indicate that a certain equilibrium value for the density is reached at prolonged depressurization times up to the point where shrinkage becomes predominant, resulting in a further increase of the density.

Finally, Figure 8 shows that the density of the produced foams under adiabatic conditions remains constant, because during these experiments, the temperature decreases to a value below the T_g and no shrinking occurs. Furthermore, cell growth is prematurely stopped due to the reverse plasticization effect, leading to densities of around 110 g/dm^3, which are slightly higher compared to the densities of the isothermally and isoperibolically foamed SMMA samples at higher depressurization rates. The effect of reverse plasticization on the produced foams is further illustrated in Figure 9. Here, the densities of the foams produced under adiabatic conditions are plotted versus the temperature. It clearly shows that at 100°C the densities of the foams are higher. This is again caused by reverse plasticization that takes place due to the cooling of the reactor during the expansion of the CO_2, leading to a temperature drop of ~20°C. At 118.5°C, the temperature drops to a value just below the T_g of the pure polymer, allowing cell growth to take place for a longer period of time before the morphology is eventually vitrified. Even though the cell growth is prematurely stopped in the adiabatic experiments, this expansion mode is still more desirable than shrinking that occurs in the isoperibolic and isothermal modes, because the adiabatic expansion allows much better control of the foam morphology.

Because of the large cell size of the produced foams, it appeared to be impossible to use a scanning electron microscope in combination with the previously developed Voronoi Analysis Method[18] for further analysis of the foam morphology. Optical microscopy has been used instead to obtain an indication of the morphology of the produced foams. Figure 10 displays the density of the adiabatically produced PS and SMMA versus pressure, together with the corresponding microscopy pictures. The pictures clearly show that the cell size decreases with the increase in pressure. This is in agreement with the experiments performed in previous studies.[3,5]

Flexibility of the polymer matrix

The temperature during the depressurization step plays an important role in the foaming process, because it is directly related to the flexibility of the polymer matrix. The temperature profile determines to a great extent whether the polymer is in the glassy or rubbery state and therefore, whether the polymer matrix will be flexible enough to allow cell growth. However, the degree of crosslinking also has an influence on the flexibility of the polymer matrix. A more crosslinked polymer matrix is more rigid, resulting in a higher resistance

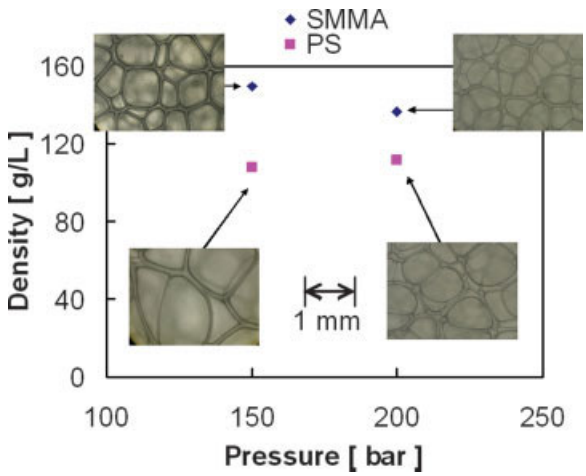

Figure 10. Optical microscopy pictures and the corresponding densities of PS and SMMA foams versus pressure, foamed at 3.2 turns of the valve and saturated at 118.5°C.

[Color figure can be viewed in the online issue, which is available at www.interscience.wiley.com.]

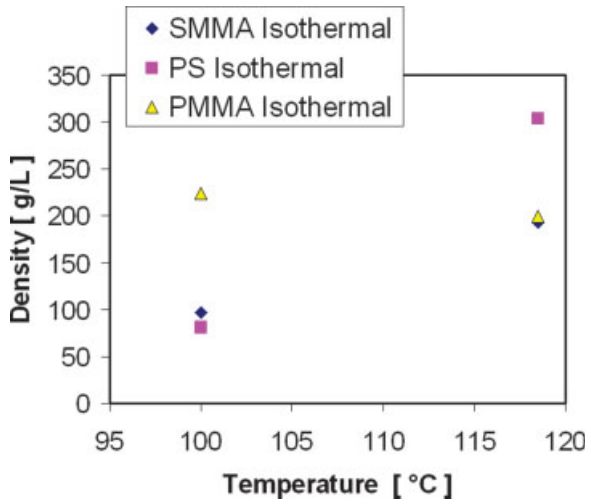

Figure 11. Density of foams produced under isothermal conditions versus the temperature foamed at three valve turns and saturated at 200 bar.

[Color figure can be viewed in the online issue, which is available at www.interscience.wiley.com.]

to cell growth. The reverse also holds a more crosslinked polymer is less susceptible to shrinking due to the rigidity of the matrix. On the basis of this, PMMA and SMMA discs are expected to display less cell growth when compared with the PS discs, because self-crosslinking occurs during the pressing of the PMMA and SMMA discs. This is confirmed by Figure 11, where the density versus the saturation temperature of the different polymers under isothermal-foaming conditions is plotted. It can clearly be seen that at 100°C, where shrinking is absent, the PS foam has the lowest density, followed by SMMA and PMMA, respectively. Furthermore, at 120°C, the PS foam has the highest density of the three polymeric foams. This is directly related to the shrinking that takes place at these conditions, which has been visually observed. Because of the higher degree of crosslinking, the exposure to higher temperatures has less effect on the foam morphology of SMMA and PMMA, resulting in less shrinkage and therefore in lower densities. These effects indicate the difference in flexibility of the polymer matrix. This is also demonstrated in Figure 9 where the relatively rigid PMMA expands less when compared with the relatively flexible PS.

Conclusions

In this article, the effects of the different temperature profiles on the foaming process and the foam morphology have been studied, for which isothermal, adiabatic, and isoperibolic-foaming experiments have been performed. The experiments show that the foaming process can be divided into four stages: a nucleation stage, a stage with slow cell growth, a stage with fast cell growth, and a shrinking stage. At the end of the isothermal and isoperibolic-foaming experiments, performed at temperatures above the T_g of the pure polymer, the shrinking stage starts to have a predominant effect on the morphology of the polymeric foams, due to the prolonged exposure to these high temperatures. This stage is absent in the foaming experiments performed at adiabatic conditions. On the basis of the results, it can be concluded that the temperature profile during the depressurization step of foaming experiments using $scCO_2$ as a foaming agent appears to have a major influence on the foam morphology.

In addition, the flexibility of the polymer matrix is another important parameter for defining the foam morphology. This flexibility is not only determined by the temperature profile of the experiment, but also by the degree of crosslinking of the polymer matrix. A more crosslinked polymer matrix increases the resistance to cell growth of the matrix. Reversely, a more crosslinked polymer is less susceptible to shrinking due to the rigidity of its matrix.

In terms of morphology control, especially the exposure to higher temperatures at the end of the foaming experiments plays an important role, because this determines the degree of shrinking that occurs. For that reason, the adiabatic mode has proven to give the best control on the foam morphology. It allows the saturation of the polymer with CO_2 at high temperature and gives flexibility to the matrix at the beginning of the depressurization step. Furthermore, because of the temperature decrease, the adiabatic mode prevents shrinking by vitrifying the produced foam morphology.

Acknowledgments

This research was supported by a grant from the Swiss National Science Foundation (number: P1012-109215 awarded to M.F. Kemmere). The financial support by SenterNovem and the Netherlands Organization for Scientific Research (NWO) is also acknowledged.

Literature Cited

1. Reed RA. New blowing agents for foaming plastics. *Br Plast Moulded Prod Trader*. 1960;33:468–472.
2. Kazarian SG. Polymer processing with supercritical fluids. *Polym Sci Ser C*. 2000;42:78–101.
3. Goel SK, Beckman EJ. Generation of microcellular polymeric foams using supercritical carbon dioxide. I. Effect of pressure and temperature on nucleation. *Polym Eng Sci*. 1994;34:1137–1147.
4. Goel SK, Beckman EJ. Generation of microcellular polymeric foams using supercritical carbon dioxide. II. Cell growth and skin formation. *Polym Eng Sci*. 1994;34:1148–1156.
5. Jacobs MA, Kemmere MF, Keurentjes JTF. Foam processing of poly(ethylene-*co*-vinyl acetate) rubber using supercritical carbon dioxide. *Polymer*. 2004;45:7539–7547.
6. Sheridan MH, Shea LD, Peters MC, Mooney DJ. Bioabsorbable polymer scaffolds for tissue engineering capable of sustained growth factor delivery. *J Controlled Release*. 2000;64:91–102.
7. Arora KA, Lesser AJ, McCarthy TJ. Preparation and characterization of microcellular polystyrene foams processed in supercritical carbon dioxide. *Macromolecules*. 1998;31:4614–4620.
8. Liang MT, Wang CM. Production of engineering plastics foams by supercritical CO_2. *Ind Eng Chem Res*. 2000;39:4622–4626.
9. Shieh YT, Liu KH. The effect of carbonyl group on sorption of CO_2 in glassy polymers. *J Supercritical Fluids*. 2003;25:261–268.
10. Alessi P, Cortesi A, Kikic I, Vecchione F. Plasticization of polymers with supercritical carbon dioxide: experimental determination of glass-transition temperatures. *J Appl Polym Sci*. 2003;88:2189–2193.

11. Zhang Z, Handa YP. An in situ study of plasticization of polymers by high-pressure gases. *J Polym Sci Part B: Polym Phys*. 1998; 36:977–982.
12. Van der Vegt NFA, Briels WJ, Wessling M, Strathmann H. The sorption induced glass transition in amorphous glassy polymers. *J Chem Phys*. 1999;110:11061–11069.
13. Hemminger W, Sarge SM. Definitions, nomenclature, terms and literature. In: Brown M, editor. *Handbook of Thermal Analysis and Calorimetry,* Vol. 1. Amsterdam: Elsevier, 1998:1–72.
14. International Confederation of Thermal Analysis and Calorimetry, 2006. http://www.ictac.org.
15. Jacobsen JP. Reaction calorimeter—a useful tool in chemical engineering. *Thermochim Acta*. 1990;160:13–23.
16. Fortini S, Lavanchy F, Meyer T. Reaction calorimetry in supercritical carbon dioxide—methodology development. *Macromol Mater Eng*. 2004;289:757–762.
17. Jacobs LJM, Danen KCH, Kemmere MF, Keurentjes JTF. A parametric study into the morphology of polystyrene-*co*-methyl methacrylate foams using supercritical carbon dioxide as a blowing agent. *Polymer*. 2007;48:3771–3780.
18. Jacobs LJM, Danen KCH, Kemmere MF, Keurentjes JTF. Quantitative morphology analysis of polymers foamed with supercritical carbon dioxide using Voronoi diagrams. *Comput Mater Sci*. 2007;38: 751–758.

Manuscript received Dec. 5, 2006, and revision received July 2, 2007.